

Experimental and Numerical Definition of the Reverse Vortex Combustor Parameters

Igor Matveev*
Applied Plasma Technologies,
Falls Church, Virginia, 22046

Serhiy Serbin†
National University of Shipbuilding,
Nikolaev, Ukraine, 54025

Theoretical and experimental investigations of a gaseous fuel burning reverse vortex combustor have been conducted. A generalized method based on numerical solution of the conservation and transport equations for multi-component, chemically reactive turbulent system was utilized. Selected models of turbulent transposition provide adequate description of the working processes in similar combustion systems with strongly swirling flows. Obtained results and recommendations can be used for the reverse vortex combustor operation modes and geometry optimization, perspective combustors for propulsion and power generation design and engineering.

I. Introduction

Theoretical investigations of working processes in vortex combustors with highly turbulent flows of air, fuel, and products of their reactions are not simple [1-4]. Due to intensive development and achieved progress in numerical solutions of the fluid dynamics and chemical kinetics equations it is now possible to model the main physical and chemical processes inside combustors that are difficult to study experimentally. That could dramatically reduce expenses required for research and development of perspective combustors.

The development of a new generation of combustion chambers should be based on better understanding of the physical and chemical processes of turbulent combustion in highly recirculating flows and ability of such combustors modeling taking in account complicity of their 3D geometry and variety of operation modes.

A reverse vortex combustor (RVC), in which aerodynamics dramatically differs from conventional direct vortex combustors has been developed on the basis of the Applied Plasma Technologies recent patent applications [5-7] and preliminary tests have been conducted. Full-scale atmospheric pressure model tests proved the concept's advantages as follows: highly efficient internal mixing of fuel and oxidizer, stable combustion with dramatically extended flammability limits, simple air swirler and fuel injectors, no cooling of the combustor walls, simple combustor design, cheaper materials for combustor fabrication, opportunity to feed fuel through the liner walls, simple conversion into the multi-fuel and multi-zone combustor.

Working processes in the novel reverse vortex combustor are similar to that in Ranque-Hilsh vortex tubes [8] used for gas-dynamic cooling. Recent attempts to simulate these phenomena using CFD were claimed to be successful [9], but careful investigation of the obtained results shows that the authors were able to simulate significant decrease of thermodynamic temperature only, but not the stagnation temperature decrease that takes place in a real device. We believe that success could be achieved on the basis of two-equation turbulence model improvement which allows calculation of the Reynolds stress or velocity co-variations as far as turbulent flows by employment of the differential transportation equations [10, 11]. Unfortunately, the effect of specific terms on the numerical stability of calculation is not known. That's why verification of these terms and more precise definition of the models empirical constants by the mathematical means and physical tests on RVC are required.

* President & CEO, 7231 Woodley Place, Falls Church, VA 22046

† Professor, Machine-Building Institute, National University of Shipbuilding, 9 Geroev Stalingrada Ave., Nikolaev, Ukraine, 54025

The objectives of current research are experimental and numerical definition of the RVC parameters and comparison of the parameters prediction for different turbulence models.

II. Mathematical Modeling

For modeling of physical and chemical processes inside the RVC a generalized method based on numerical solution of the combined conservation and transport equations for multi-component chemically reactive turbulent system was employed. This method provides a procedure of the sequential numerical integration of the differential equations which describe reacting viscous gas flows. A 3D model of stationary and non-stationary reacting flows [1-4, 12] has been utilized which allows to predict plasma-chemical influence and optimize parameters of the combustors taking into consideration mixing, turbulence, radiation and combustion features.

Modeling of physical and chemical processes in the reverse vortex combustor is based on solution of the well-known system of the differential equations of mass, impulse and energy conservation for the multi-component, turbulent, chemically reacting system [1-3] in the following way:

- the mass conservation equation

$$\frac{\partial \rho}{\partial t} + \nabla \cdot (\rho u) = \rho^s,$$

- the momentum conservation equation

$$\frac{\partial (\rho u)}{\partial t} + \nabla \cdot (\rho u u) = -\nabla p - \nabla \left(\frac{2}{3} \rho k \right) + \nabla \cdot \sigma + F^s + \rho g,$$

- the continuity equation for species m

$$\frac{\partial \rho_m}{\partial t} + \nabla \cdot (\rho_m u) = \nabla \cdot [\rho D \nabla \left(\frac{\rho_m}{\rho} \right)] + R_m + S_m,$$

- the internal energy equation

$$\frac{\partial (\rho I)}{\partial t} + \nabla \cdot (\rho u I) = -\rho \nabla \cdot u - \nabla \cdot J + \rho \varepsilon + \dot{Q}^c + \dot{Q}^s,$$

- the turbulent kinetic energy transport equation

$$\frac{\partial \rho k}{\partial t} + \nabla \cdot (\rho u k) = -\frac{2}{3} \rho k \nabla \cdot u + \frac{\sigma}{\nabla u} + \nabla \cdot \left[\left(\frac{\mu}{Pr_k} \right) \nabla k \right] - \rho \varepsilon + \dot{W}^s,$$

- the dissipation rate of the turbulent kinetic energy transport equation

$$\frac{\partial \rho \varepsilon}{\partial t} + \nabla \cdot (\rho u \varepsilon) = -\left(\frac{2}{3} C_{\varepsilon_1} - C_{\varepsilon_3} \right) \rho \varepsilon \nabla \cdot u + \nabla \cdot \left[\left(\frac{\mu}{Pr_\varepsilon} \right) \nabla \varepsilon \right] + \frac{\varepsilon}{k} \left[C_{\varepsilon_1} \frac{\sigma}{\nabla u} - C_{\varepsilon_2} \rho \varepsilon + C_s \dot{W}^s \right].$$

The above mentioned equations are written down in the vectorial form for which operator

$$\nabla = i \frac{\partial}{\partial x} + j \frac{\partial}{\partial y} + k \frac{\partial}{\partial z},$$

and the fluid velocity vector

$$u = u(x, y, z, t)i + v(x, y, z, t)j + w(x, y, z, t)k,$$

where i, j, k are the unit vectors in the x, y, z directions.

In these equations t is the time; ρ , the mass density of the mixture; ρ^s , the source term due to the spray of liquid; p , the fluid pressure; k , the turbulent kinetic energy; σ , the viscous stress tensor; F^s , the rate of rise in momentum; g , the specific body force; ρ_m , the mass density of species m ; D , the diffusion coefficient; R_m, S_m , the source terms due to chemistry and dispersed phase; I , the specific internal energy; J , the heat flux vector; \dot{Q}^c, \dot{Q}^s , the source terms due to chemical heat release and spray interactions; μ , the coefficient of viscosity; $C_{\varepsilon_1}, C_{\varepsilon_2}, C_{\varepsilon_3}, Pr_k, Pr_\varepsilon$, constants; \dot{W}^s , the source term due to interaction with the spray.

We have to note, that in circulating flows turbulence viscosity factor is anisotropic. That's why application of a standard k - ε - turbulence model could be not efficient. For that cases an RNG k - ε - model could be applied [13]. The RNG-based k - ε - turbulence model is derived from the instantaneous Navier-Stokes equations, using a mathematical technique called "renormalization group" (RNG) methods. For strongly recirculating flows, in devices similar to cyclones, an appropriate Reynolds stress model should be selected [1, 11].

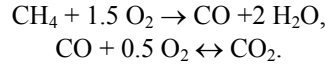
The Reynolds stress model (RSM) involves calculation of the individual Reynolds stresses $\overline{u_i' u_j'}$ using differential transport equations. The individual Reynolds stresses are then used to obtain closure of the Reynolds-averaged momentum equation. The exact form of the Reynolds stress transport equations may be derived by taking moments of the exact momentum equation. This is a process wherein the exact momentum equations are multiplied by a fluctuating property, the product then being Reynolds-averaged.

The source of chemical species m due to reaction R_m is computed as the sum of the reaction sources over the k reactions

$$R_m = \sum_k R_{mk},$$

where R_{mk} is the rate of creation (destruction) of species m during reaction k .

Combustion in gaseous phase is modeled as two-step chemical reactions:



Reaction rate is calculated considering both the Arrhenius, and Magnussen and Hjertager models:

$$R_{mk} = \nu_{mk} M_m T^{\beta_k} A_k \prod_j [C_j]^{v_{jk}'} \exp(-E_k / RT), \quad R_{mk} = A \rho \frac{\varepsilon X_m}{k \nu_{mk}},$$

where ν_{mk} is the stoichiometric coefficient; M_m , the molecular weight of species m ; β_k , the temperature exponent; A_k , the pre-exponential factor; C_j , the molar concentration of each species j ; v_{jk}' , the concentration exponent; E_k , the activation energy; R , the gas constant; A , empirical constant; X_m , the mass fraction of chemical species m .

The reaction rate is taken to be the smaller of two these expressions. This chemistry- turbulence approach is used because there are regions within the reverse vortex combustor where the turbulent mixing rate is faster than the chemical kinetics (low temperature regions in the vicinity of the fire tube walls, axial and radial inlets).

The boundary conditions in the axial and radial inlets, symmetry axes, walls and outlet from a RVC were set in accordance with the conditions for carrying out physical experiments and recommendations for modeling the turbulent burning processes. The method for the system solution, the finite difference scheme and the solution stability analysis are explained in detail in [2-4, 12, 13].

III. Test Design and Preliminary Calculations

A. Experimental Setup

A full-scale atmospheric pressure model of the reverse vortex combustor is shown in Fig. 1. It has an internal diameter of 145 mm and length of 240 mm. Air comes into combustor through the swirler with tangential channels, located in the area of exit nozzle, which diameter in experiments was varied from 39 to 130 mm. Gaseous fuel was fed through two orifices at the bottom of the RVC, which were located symmetrically to the combustor axis on diameters respectively 62, 92 and 124 mm. A special nozzle for gaseous fuel injection was utilized for central fuel feeding. The flexible combustor design provided fast and simple replacement of the carbon steel shell on quartz tubing for the process visualization. Air flow rate through combustor was smoothly regulated from 0 to 20 g/s. Both air and fuel regulations provided wide range of the combustor operation modes with equivalence ratios from 0.05 to 0.95. Measurements of the combustor walls and the exhaust gases temperature were conducted by six type K thermocouples, and special assembly of six thermocouples located downstream the flow in the nozzle's cross section (Fig. 2).

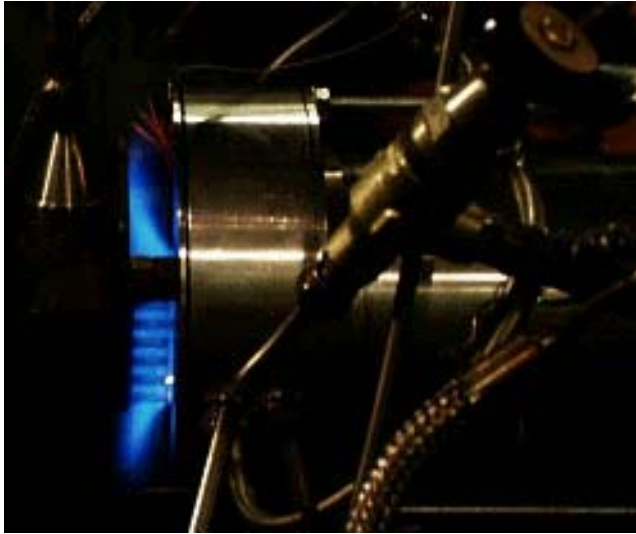


Figure 1. Reverse vortex combustor in operation.

No one of the combustor parts, including nozzle had specially organized cooling. Fuel and air mixing took place in the central part of the combustor due to spatial and spiral flow after the air U-turn in the bottom area. These flow lines could be clearly seen in Fig.3. As appeared, the exit nozzle ID defines the combustion zone OD. The visible combustion zone external diameter is close to the nozzle internal diameter. This requires appropriate location of the fuel injectors and their parameters to provide effective mixing and efficient chemical reacting. Similar method of the propellants mixing and burning process organization appears effective both from the point of view fuel combustion completeness, and

in Fig.3. As appeared, the exit nozzle ID defines the combustion zone OD. The visible combustion zone external diameter is close to the nozzle internal diameter. This requires appropriate location of the fuel injectors and their parameters to provide effective mixing and efficient chemical reacting. Similar method of the propellants mixing and burning process organization appears effective both from the point of view fuel combustion completeness, and

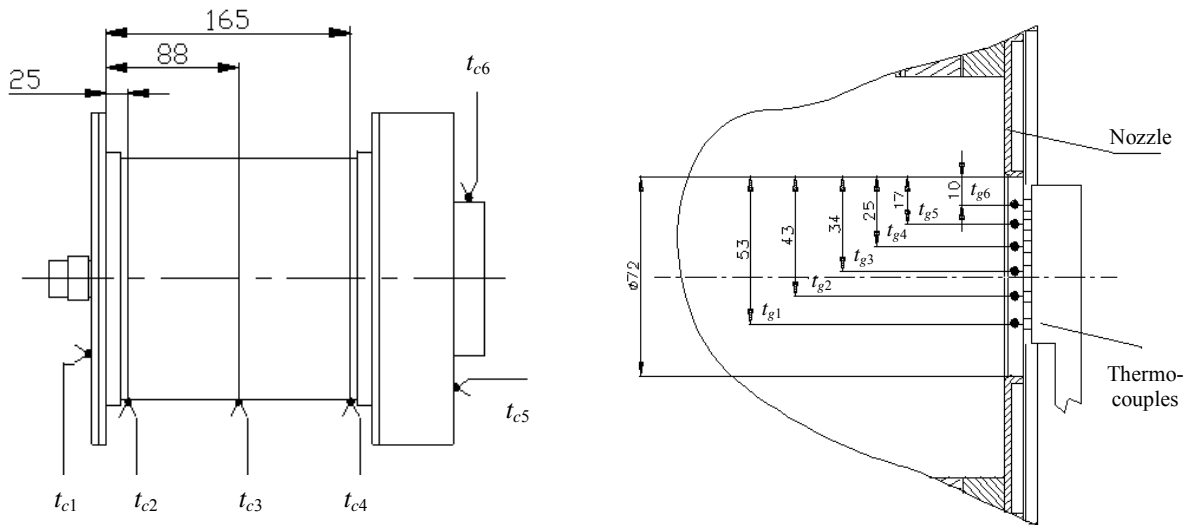


Figure 2. The scheme of wall and exit temperature measurements in the RVC.

low walls temperature of all RVC elements. The experimental data of the combustion chamber walls temperature obtained under varying of equivalence ratios are shown in Fig. 4. The first series (left figure) corresponds to fuel

flow rate 0.147–0.43 g/s, and the second (right figure) – to flow rate 0.226–1.007 g/s. It is evident that the maximum temperatures take place at the exit nozzle area and do not exceed 370 °C that testifies to effective cooling organization of all the RVC parts.

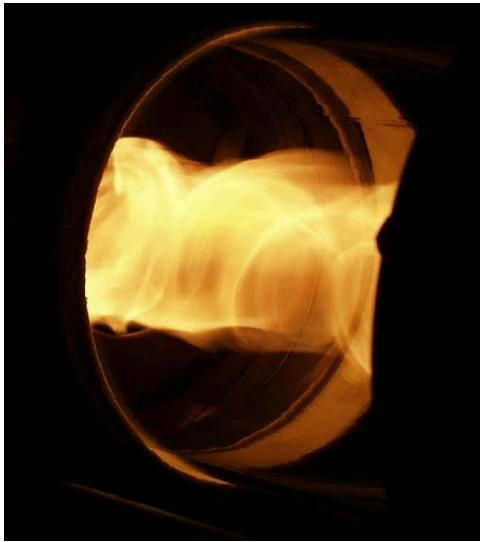


Figure 3. Visualization of the swirling reacting flow in RVC.

B. Preliminary Theoretical Results

Achieved promising experimental data and their comparison with the computation 3D-CFD modeling results even for the simplest combustion design showed significant discrepancy for the major selected flow models.

Fig. 5 presents preliminary calculation results of the flow axial velocity profiles (the upper bound is 11 m/s, the maximum negative value - 7 m/s) in the meridian cross section of the RVC for the air flow rate 12 g/s employing different turbulence models: a) k-ε turbulence model; b) RNG k-ε model; c) Reynolds Stress Model (RSM). Visible difference proves significant dependence of the flow structure and vortex formation parameters on the calculation model selection.

Conducted calculations showed significant influence of the air circulation degree (air was fed through four tangential channels) and its input velocity, RVC geometry, place of the fuel feeding. Spatial distribution of the components concentration and temperature changes dramatically depending on turbulence degree and the reagents mixing quality. Turbulence, as a mechanism of the moles mixing, determines contact between molecules of the gaseous fuel and oxidizer,

affects on the flame propagation velocity and heat transfer enhancement. More over, it defines chaotic mixing of the gaseous moles which leads to appearance of continuous and irregular pulsations of velocity, temperature and the reagents concentration in all flow point.

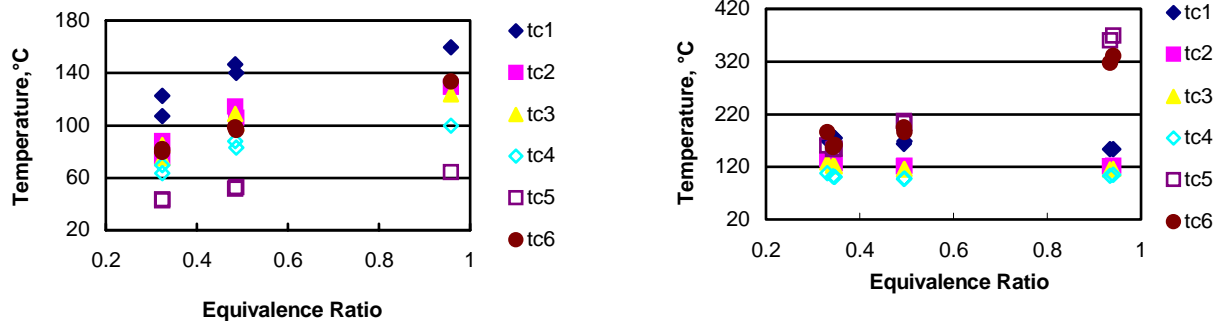


Figure 4. Dependence of the wall temperature on equivalence ratio.

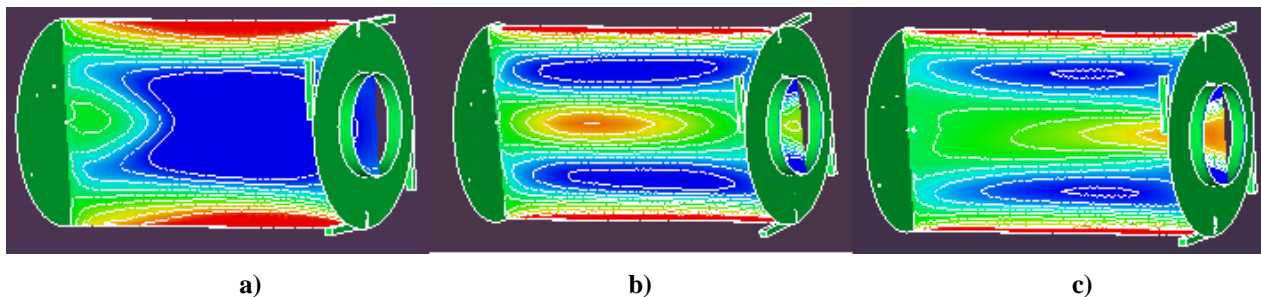


Figure 5. Contours of cold flow axial velocity in 3D model of the reverse vortex combustor.

Fig. 6 shows the temperature contours of the reverse vortex (RV) flow in the case of gaseous fuel diffusion combustion (total combustion zone temperature is about 2200 K) with fuel feeding through two symmetric holes on the ID = 62 mm for equivalence ratio 0.43 and simplest Eddy-Dissipation combustion model employing different turbulence models: a) k- ϵ (Fig. 6a) and RSM (Fig. 6b). The RSM model provides the closest to experimental data results for the walls temperature and exhaust gases temperature fields. Nevertheless, the discrepancy between the measured data and CFD analyses was more than 20 % for near stoichiometric combustion modes. The main reason of so high level of error could be in significant spatial variation of the propellants characteristics inside the RVC. It could be also related to difficulties in calculation of the non-linear velocities of chemical reactions and influence of turbulence which is much stronger in RV flow. We have also to note that standard k- ϵ turbulence model gives the worst results in our case.

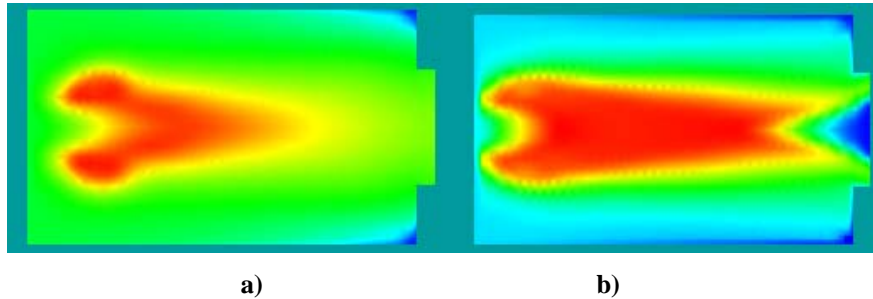


Figure 6. Temperature contours in axial cross-section of the reverse vortex combustor.

Kinetic energy of turbulence in case of RVC has the upper bounds in the areas of tangential air input, central fuel feeding, near walls and in the combustor's center, where the velocity component gradients are significant. Such a kinetic energy distribution in the central vortex zone could be explained by the centrifugal effect influence and the turbulent diffusion. The values of turbulent pulsations are mainly depending on initial level of the velocity pulsations in the entry cross sections.

Temperature distribution is an evidence of a complex aerodynamic flow structure inside the RVC. Fig. 7 shows comparison of the actual and predicted (dotted and firm lines) radial gas temperature contours at the combustors outlet. Actual temperatures have been measured simultaneously by six thermocouples located on radiuses -17, -7, 2, 11, 19 and 26 mm (see Fig. 2). Fuel was fed into the combustor through two co-axial holes on radiuses of 46 mm. Predicted data were obtained for the k- ϵ and RNG k- ϵ turbulence models and gaseous fuel diffusion combustion

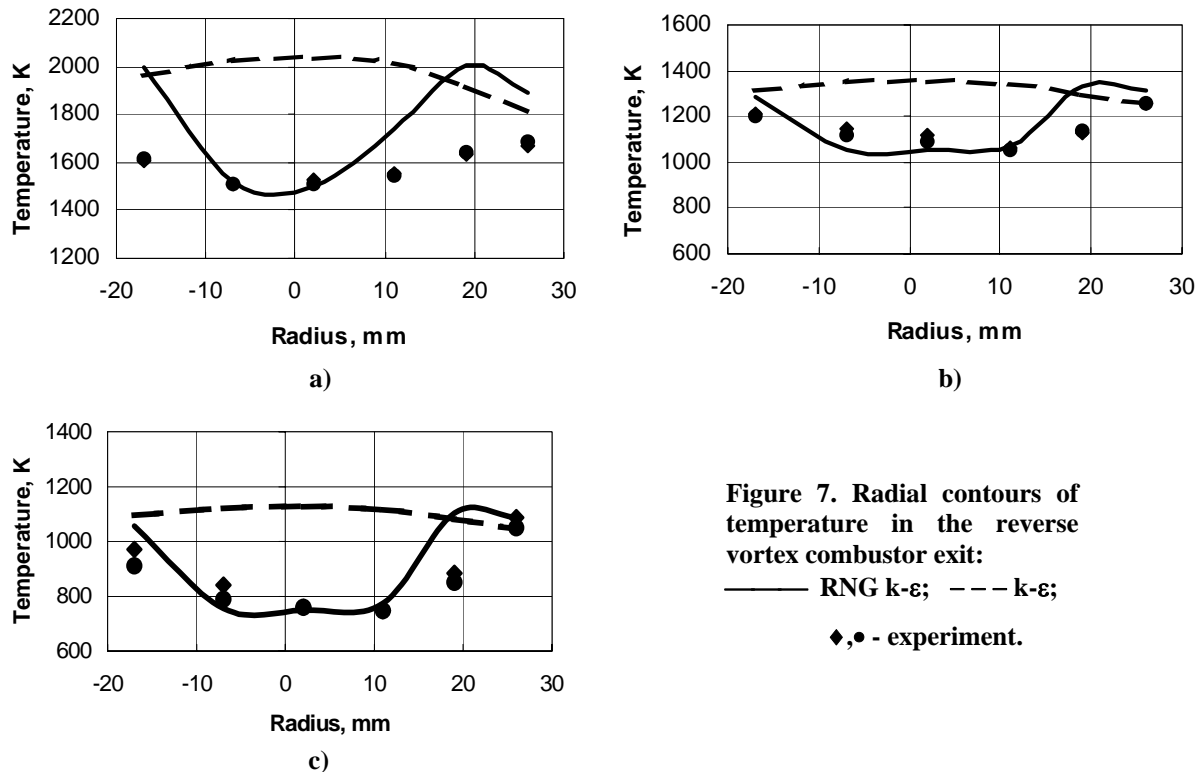


Figure 7. Radial contours of temperature in the reverse vortex combustor exit:
 ——— RNG k- ϵ ; - - - k- ϵ ;
 ◆, ● - experiment.

assumption. Fig. 7a reflects the combustion chamber mode with equivalence ratio 0.67, Fig. 7b – 0.38, and Fig. 7c – 0.29.

Experiments clearly demonstrate a reverse flow zone in a near axis area of the outlet nozzle. This zone becomes more visible while running RVC on the lean mixture operation modes. Radial temperature contours have significant uniformity in those cases. Difference between maximum and minimum temperature values reaches 200 and more degrees. This could be explained by exhaust gases dilution with an ambient air injection into the pre-axis zone. Numerical simulation on the basis of standard k-ε turbulence model provides relatively uniform outlet temperature profile with maximum on the axis. That conflicts with the experiments. An improved RNG k-ε turbulence model gives more realistic results, however for near stoichiometric mixtures, qualitative discrepancy remains significant.

IV. Theoretical Investigations

C. Mathematical Model Selection

Preliminary calculations have shown significant dependence of the RVC working process parameters from turbulence and burning model characteristics. Besides, presence of the backflow in the exit nozzle area, which was confirmed experimentally and theoretically, does not allow accurate prediction of concentration, temperatures and velocities distribution in the area of gas exhaust into atmosphere in case of using only inside chamber difference mesh. The combustion products are considerably diluted with air, which is injected from atmosphere, and, therefore, the flow structure inside the combustor additionally depends on characteristics of the flow and mixing processes outside the exhaust nozzle. Therefore, a computational three-dimensional mesh was modified. In addition to the primary mesh the new region was added after the combustor's exit nozzle. That has allowed the processes consideration, which accompany rotating flows in the combustor exit.

With the purpose of the most realistic turbulence model selection some calculations of the combustion parameters in RVC were conducted for the follows conditions: equivalence ratio $\phi = 0.66$, that corresponds to air flow rate of 14.41 g/s and gaseous fuel flow rate of 0.695 g/s, for fuel feeding through two orifices on 92 mm diameter (Fig. 8). Three models of turbulence were applied - standard k-ε model, RNG k-ε model, and RSM model. In burning methane-air calculations a generalized finite rate model was used. This approach is based on solution of

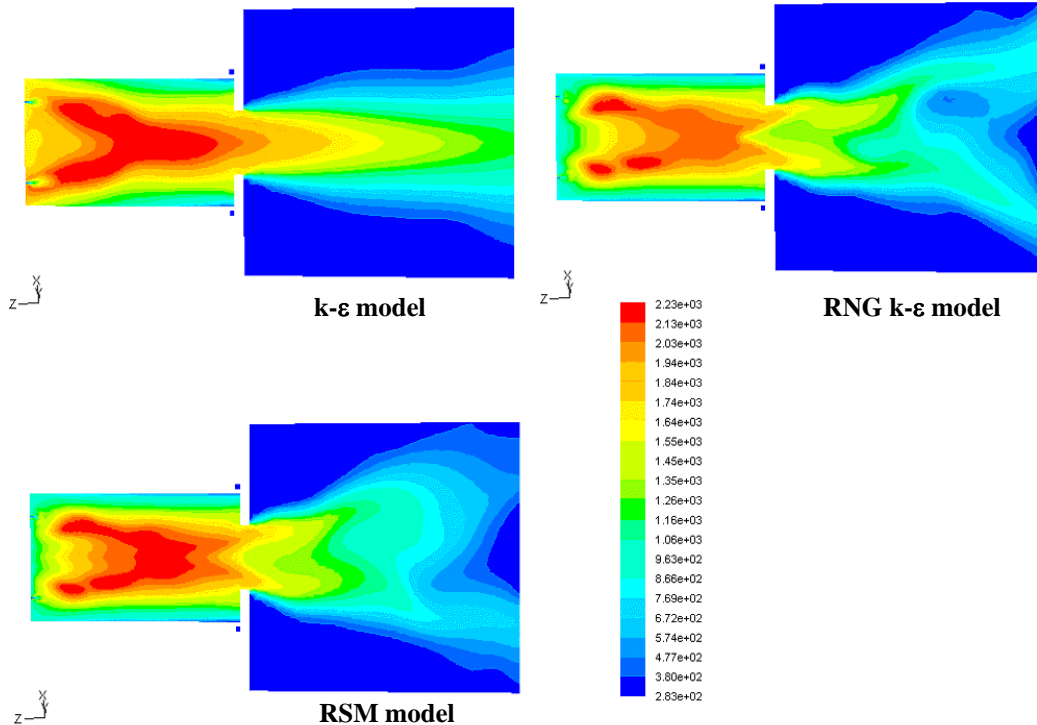


Figure 8. Contours of static temperature in the RVC axial cross-section.

the transport equations for the species mass fractions with chemical reaction mechanism. The reaction rates, which appear as the source terms in the species transport equations are computed from Arrhenius finite rate (FR) expressions, or from the eddy-dissipation model (EDC) with detailed chemical kinetics incorporated in turbulent flames. Notice, that models of this type are suitable for a wide range of applications, including premixed, partially premixed, and non-premixed turbulent combustion. In the RVC case most frequently for comparative calculations the eddy-dissipation model was used. Reaction rates were assumed to be controlled by the turbulence, so expensive Arrhenius chemical kinetic calculations can be avoided. The model is computationally cheap and only two-step heat-release mechanisms for methane combustion were required.

The contours of static temperature in RVC axial cross-section for three considered turbulence models using ED combustion model with standard wall functions are indicated in Fig. 8. It is obvious, that standard $k-\epsilon$ model does not allow adequately describe a swirled air jet distribution in the cylindrical combustor wall region. It is washed away very fast, and depth of its active penetration into the RCV near-wall layers does not exceed half of the liner's length. Significant wall temperatures at the combustor's bottom area (1800-1900 K) contradict with experimental data (see Fig. 4). Besides, the air backflows at the axial part of the exit nozzle do not exist at all. That does not correspond to actual aerodynamic structure. The RNG $k-\epsilon$ and RSM models give more realistic flow structure that qualitatively continuous to experiment. In both cases the swirling air stream reaches the combustor's bottom and participates in further forming of the central whirlwind with diameter compared to the exit nozzle diameter. Temperature distribution in the nozzle exit is modified in correspondence with a mixing particularity at the downstream calculation region (right parts of the figures).

The aerodynamic flow structure parameters calculated by three above mentioned turbulence models are very different. Dependences of temperature and velocity magnitude from the RVC length in Fig. 9 illustrate this point. It can be seen that the $k-\epsilon$ model gives considerably higher axial temperatures and velocities of the working substance in comparison with other models. The model does not also show continuation of the fuel burning within the combustor limits for some operation modes that was observed while tests. Thus, the simplest model can be eliminated from the consequent analysis.

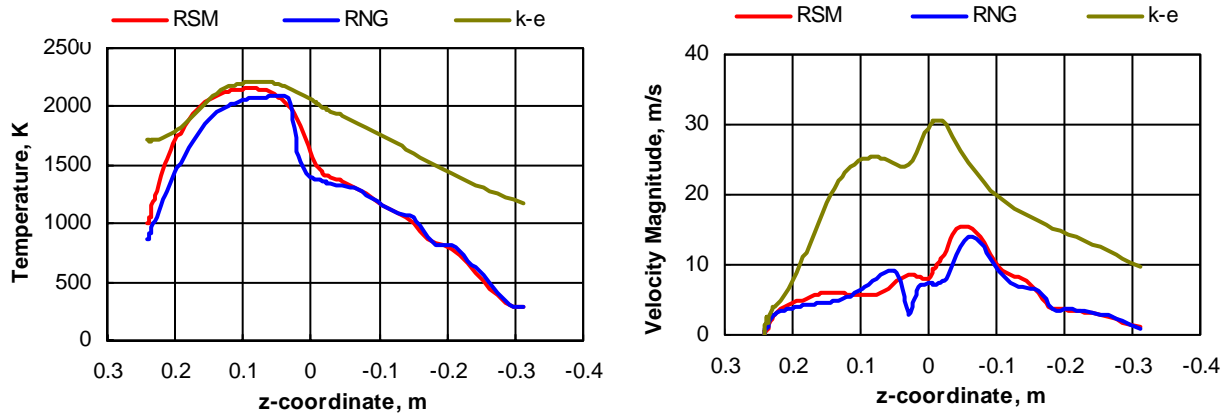


Figure 9. Dependences of temperature and velocity magnitude from the combustor length.

Comparison of the calculated and measured radial temperature contours at the reverse vortex combustor exit (Fig. 10) testifies adequacy of various combustion models. As a result, combination of the RSM turbulence model and the eddy dissipation combustion model can be considered as the most acceptable. In RVC most gaseous fuels are fast burning, and the overall rate of reaction is controlled by turbulent mixing. Employment of the more complicated models, as eddy dissipation with finite rate model (ED+FR) and EDC with chemical kinetics does not increase calculation accuracy, but requires more detailed development of the chemical equations scheme.

D. Theoretical Results and comparison with visualization data

The combustion chamber operation mode has a dominant influence on the flow aerodynamic structure and the gaseous fuel combustion process. Fig. 11 presents contours of the oxygen mass fraction in the RVC cross-section for three equivalence ratios $\phi = 0.935$, 0.495 , and 0.349 . In all cases the air flow rate was 17.8 g/s and fuel was fed

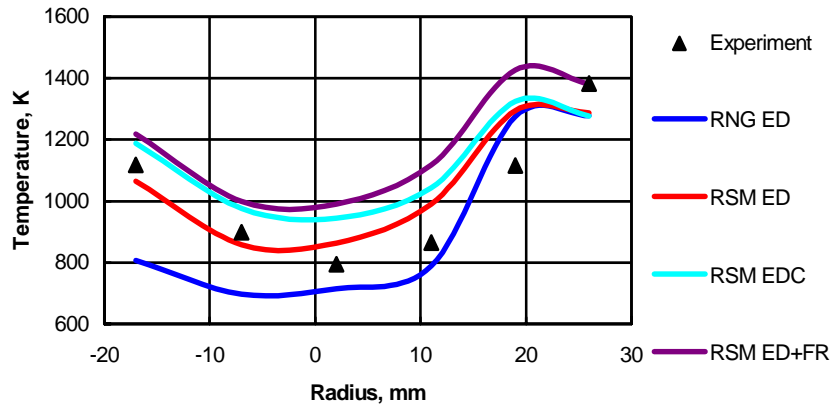


Figure 10. Radial contours of temperature in the reverse vortex combustor exit.

through two orifices symmetrically located on a diameter of 62 mm on the combustor bottom. The RSM turbulence model and the eddy dissipation methane-air, two step kinetic model were used for calculations. It could be seen that in accordance to a fuel-air mixture dilution the fuel burning out is completed within the combustor volume limits. Significant oxygen mass fractions in sections, which immediately follow exhaust nozzle, testify this fact. For practically stoichiometric mixture ($\phi = 0.935$) fuel has no enough time to finish chemical reacting completely inside the combustor, and burns down in atmosphere. For all calculated modes areas were observed along the combustor walls (cylindrical part, bottom and exit nozzle) with high oxygen mass fractions. This fact explains effective walls cooling, which was clearly observed in experiments.

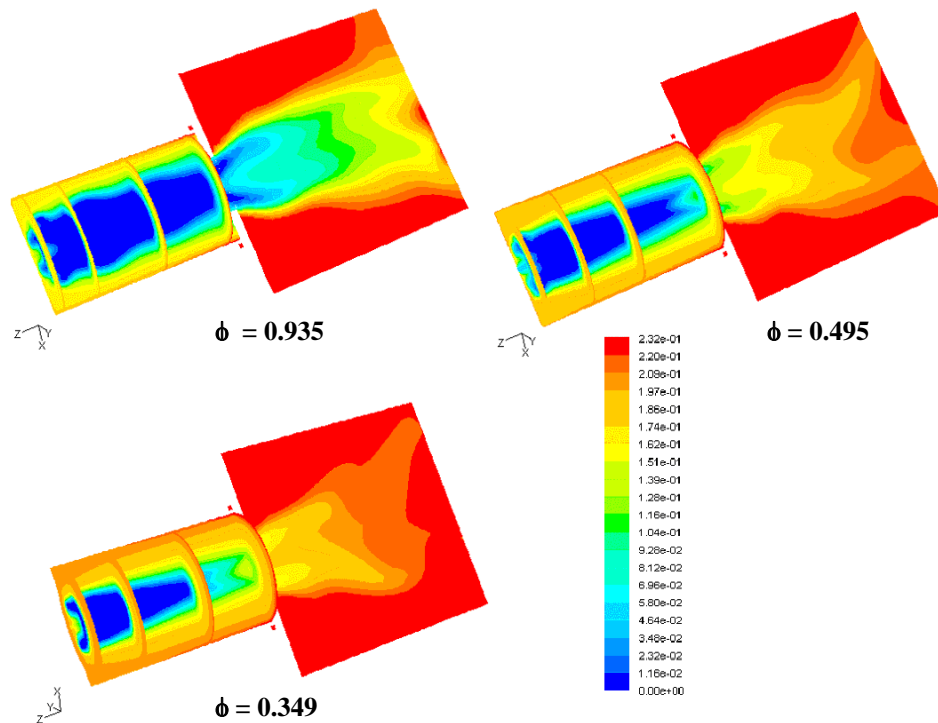


Figure 11. Contours of oxygen mass fraction in the RVC cross-section.

Fig. 12 presents pictures of the flow structure in reverse vortex combustor for three modes (a, b, c) of its work appropriate to Fig. 11 modes. Very good qualitative correlation of experimental and calculated data on form, diameter and length of burning fuel front in the RVC for different equivalence ratio is evident.

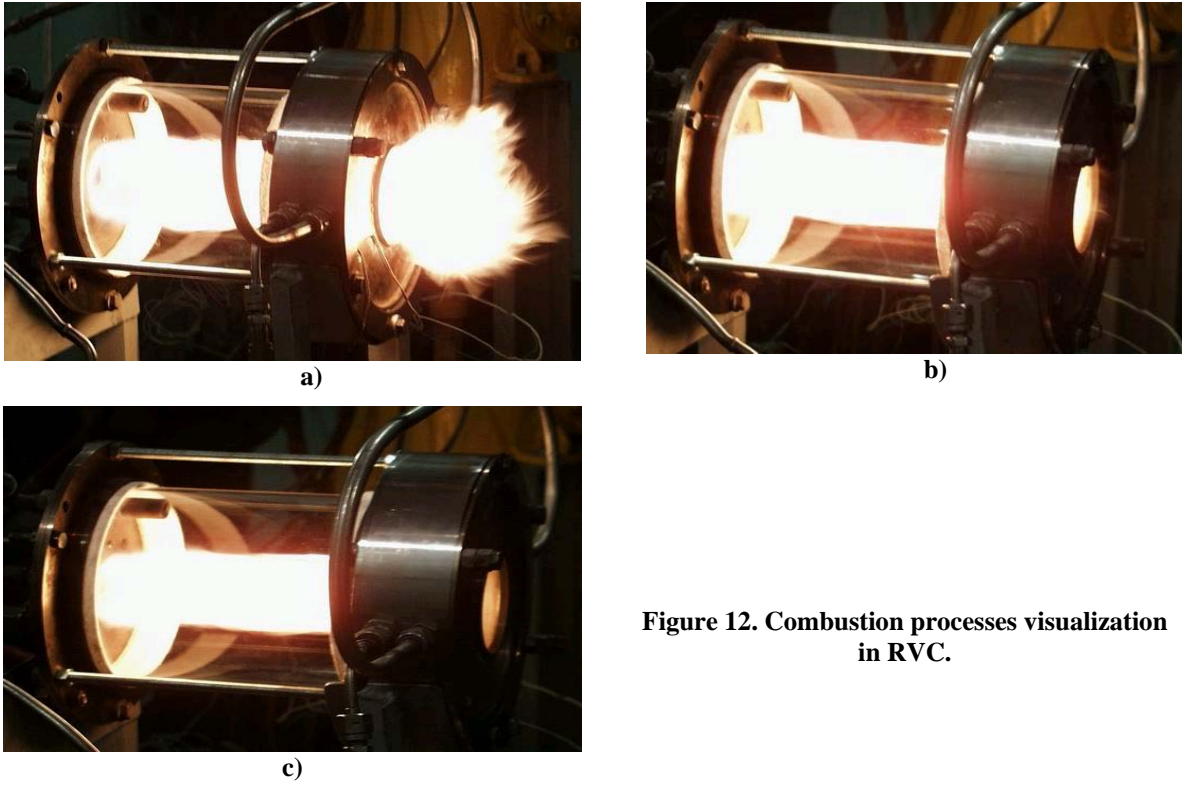


Figure 12. Combustion processes visualization in RVC.

It is interesting to monitor the fuel feeding location influence on the working process characteristics and flow structure in RVC. Fig. 13 shows contours of static temperature in the RVC axial cross-section for three different variants of fuel feeding: through two symmetric orifices located on diameters of 124 and 62 mm accordingly, and

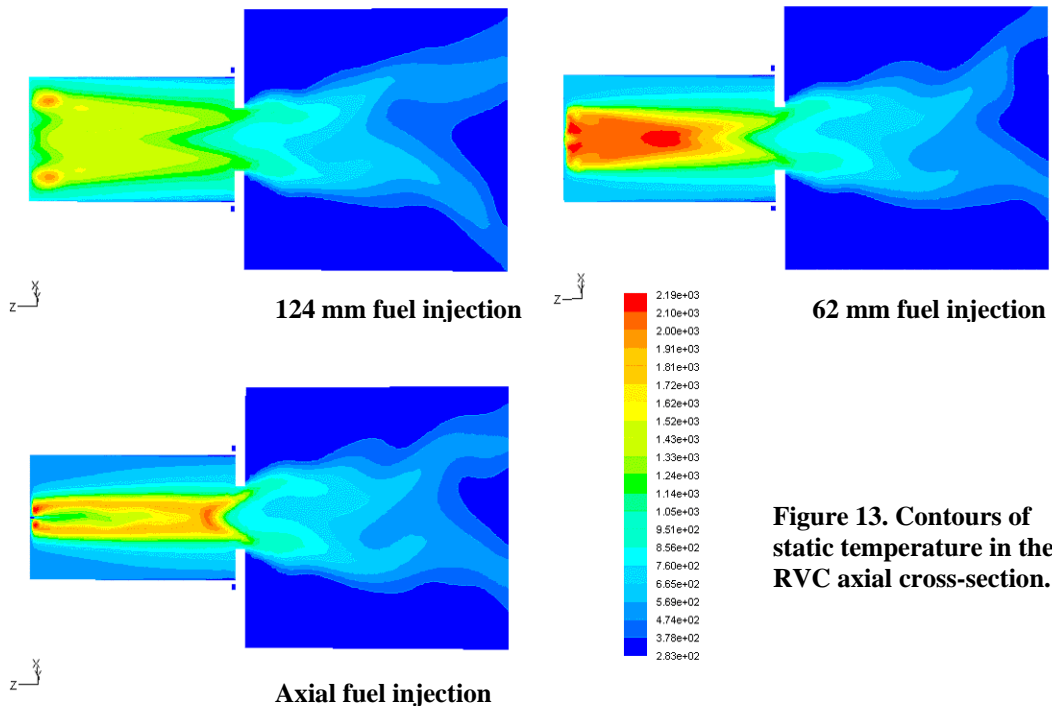


Figure 13. Contours of static temperature in the RVC axial cross-section.

through the central nozzle. Calculations were performed by the RSM turbulence model and the eddy dissipation methane-air two-step kinetics model for the air flow rate of 17.56 g/s and fuel flow rate of 0.366 g/s. The highest stability of the burning process is peculiar for the central fuel injection. In experiments with fuel feeding through the central nozzle the torch blow-out was observed in very lean mixtures zone with equivalence ratio $\phi = 0.053-0.059$, that testifies about not sufficient mixing processes quality. The calculations confirm this fact: the maximum gas temperatures are observed downstream, closer to the combustor exit.

Dependences of temperature and velocity magnitude from the combustor length are shown in Fig. 14. Maximum axial gas temperatures (near 2000 K) can be reached at the distance of 35–40 mm from the exit nozzle cross-section. Further sharp decrease is caused by the fuel burning outside the combustor.

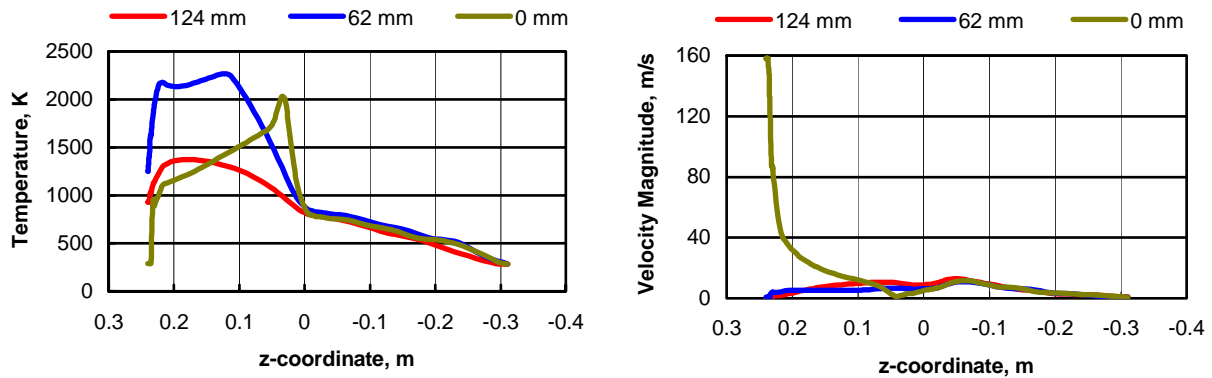


Figure 14. Dependences of temperature and velocity magnitude from the combustor length.

The most rational is the fuel injection through two orifices, symmetrically located on the diameter of 124 mm. In this case effective mixing of the injected fuel with swirling air flow and active fuel burning out take place. The flame front surface is also the biggest among tested versions.

V. Conclusion

Conducted experimental and theoretical investigations demonstrated the modeling opportunity for the complex aerodynamic flows with chemical reactions in reverse vortex combustors, revealed weak sides of the existing turbulence and combustion models for parameters prediction and determined the main directions for computation models and the reverse vortex combustor improvements.

Acknowledgments

The authors would like to acknowledge Dr. Alexander Gutsol from Drexel University for his introduction into the reverse vortex flow investigations and Dr. Thomas A. Butcher, Brookhaven National Laboratory, for cooperation and valuable discussions of the flows structure computer modeling in isothermal and chemical reaction conditions. We would like also to thank personnel of the Zaporozhie Design Bureau “Progress” in Ukraine for hosting the combustor preliminary tests.

References

- ¹Launder B. E., Spalding D. B., *Lectures in Mathematical Models of Turbulence*. Academic Press, London, 1972.
- ²Jones W.P., Priddin C.H., “Predictions of the Flow Field and Local Gas Composition in Gas Turbine Combustors”, *Seventeenth Symp. (Int.) on Combustion*, Pittsburgh, 1978, pp. 399-409.
- ³Mador R.J., Roberts R. A., “Pollutant Emissions Prediction Model for Gas Turbine Combustors”, *AIAA Paper*, 1978, No. 998, pp. 1-14.
- ⁴Spalding D.B., “Mathematical Models of Turbulent Flames: A Review”, *Combustion Science and Technology*, 1976, Vol. 13, pp. 3-35.
- ⁵Matveev, I., US Patent Application # 60/602,185 for a “Reverse Vortex Reactor with Spatial Arc”, filed 17 August 2004.
- ⁶Matveev, I., Gutsol, A., US Patent Application # 60/617,861 for a “Reverse Vortex Combustion Chamber”, filed 13, October 2004.
- ⁷Matveev, I., US Patent Application for a “Plasma Assisted Combustion System”, filed 24, December 2004.

⁸Gutsol A.F., "The Ranque effect", *Physics - Uspekhi*, 1997, Vol. 40, No. 6, pp. 639 - 658.

⁹Bezprozvannykh V., Mottl H., "The Ranque-Hilsch effect: CFD modeling", *CFD 2003: The Eleventh Annual Conference of the CFD Society of Canada*, Vancouver, BC, May 28-30, 2003, <http://tetra.mech.ubc.ca/CFD03/papers/paper30PA1.pdf>.

¹⁰Gibson M.M., Launder B. E., "Ground Effects on Pressure Fluctuations in the Atmospheric Boundary Layer", *J. Fluid Mech.*, Vol. 86, 1978, pp. 491-511.

¹¹Launder B. E., Reece G. J., Rodi W., "Progress in the Development of a Reynolds-Stress Turbulence Closure", *J. Fluid Mech.*, Vol. 68(3), 1975, pp. 537-566.

¹²Serbin S.I., "Modeling and Experimental Study of Operation Process in a Gas Turbine Combustor with a Plasma-Chemical Element", *Combustion Science and Technology*, Vol. 139, 1998.

¹³Choudhury D., "Introduction to the Renormalization Group Method and Turbulence Modeling", Fluent Inc. Technical Memorandum TM-107, 1993.